https://doi.org/10.5194/egusphere-2024-3584
Preprint. Discussion started: 29 November 2024

Driving factors of aerosol acidity: a new hierarchical quantitative analysis framework and its application in Changzhou, China

Xiaolin Duan[1,#], Guangjie Zheng[1,#,*], Chuchu Chen[1,*], Qiang Zhang[2,*], Kebin He[1]

[1] State Key Joint Laboratory of Environmental Simulation and Pollution Control, School of Environment, Tsinghua University, Beijing 100084, China
[2] Ministry of Education Key Laboratory for Earth System Modeling, Department of Earth System Science, Tsinghua University, Beijing, China.

[#] These authors contributed equally.

Correspondence to: G. Zheng (zgj123@mail.tsinghua.edu.cn); C. Chen (chencc3@mail.tsinghua.edu.cn); Q. Zhang (qiangzhang@tsinghua.edu.cn)

Abstract. Aerosol acidity (or pH) plays a crucial role in atmospheric chemistry, influencing the interaction of air pollutants with ecosystems and climate. Aerosol pH shows large temporal variations, while the driving factors of chemical profiles versus meteorological conditions are not fully understood due to the intrinsic complexity. Here, we propose a new framework to quantify the factor importance, which incorporated interpretive structural modelling approach (ISM) and time series analysis. Especially, a hierarchical influencing factor relationship is established based on the multiphase buffer theory with ISM. Long-term (2018 to 2023) observation dataset in Changzhou, China is analyzed with this framework. We found the pH temporal variation is dominated by the seasonal and random variations, while the long-term pH trend varies little despite the large emission changes. This is an overall effect of decreasing $PM_{2.5}$, increasing temperature, and increased alkali-to-acid ratios. Temperature is the controlling factor of pH seasonal variations, through influencing the multiphase effective acid dissociation constant K_a^*, non-ideality c_{ni} and gas-particle partitioning. Random variations are dominated by the aerosol water contents through K_a^* and chemical profiles through c_{ni}. This framework provides quantitative understanding on the driving factors of aerosol acidity at different levels, which is important in acidity-related process studies and policy-making.

Short summary: Aerosol acidity is an important parameter in atmospheric chemistry, while its driving factors, especially chemical profiles versus meteorological conditions, are not yet fully understood. Here, we established a hierarchical quantitative analysis framework to understand the driving factors of aerosol acidity on different time scales. Its application in Changzhou, China revealed distinct driving factors and corresponding mechanisms of aerosol acidity from annual trends to random residues.

https://doi.org/10.5194/egusphere-2024-3584
Preprint. Discussion started: 29 November 2024

1. Introduction

Aerosol acidity strongly influences particle mass and chemical constituents by regulating thermodynamic and chemical kinetic processes (Cheng et al., 2016; Pye et al., 2020; Su et al., 2020; Tilgner et al., 2021; Zheng et al., 2020). It is therefore an important parameter in the atmosphere for assessing the impact of atmospheric aerosols on human health, ecosystems and climate (Nenes et al., 2021; Pye et al., 2020). As direct measurements of aerosol pH in real atmosphere remain unavailable, thermodynamic models are widely adopted to estimate aerosol acidity and investigate its influencing factors (Clegg et al., 2001; Fountoukis and Nenes, 2007; Tao and Murphy, 2021; Zaveri et al., 2008; Zuend et al., 2008).

Driving factors of aerosol pH, especially the relative importance of chemical profiles versus meteorological conditions, have been widely investigated but still not fully understood. For example, based on long-term observations at six Canadian sites, Tao et al. (Tao and Murphy, 2019) found that temperature largely regulates the aerosol pH in summer, which the chemical profiles may also play a role in winter. Ding et al.(Ding et al., 2019) employed controlled variable tests with the thermodynamic model and concluded that in the North China Plain, sulfate, total ammonia and temperature are the common drivers of pH variations, while total nitrate barely influence the pH. In comparison, Zhou et al. (Zhou et al., 2022) demonstrated that in the Yangtze River Delta region, non-volatile cations (NVCs, including Na^+, Ca^{2+}, K^+ and Mg^{2+}) and sulfate are crucial for annual pH trends, while the seasonal and diurnal variations are determined by meteorological conditions of temperature and RH. Nevertheless, an in-depth investigation into the underlying mechanisms and quantitative attributions of how the meteorology or chemical compositions would influence the aerosol pH is still lacking.

Following the Air Pollution Prevention and Control Action Plan in 2013, the Chinese government continued to introduce the Three-Year Action Plan to Fight Air Pollution (hereinafter referred to as the Action Plan) in 2018. With the implementation of these action plans, both the $PM_{2.5}$ concentration and its chemical components have changed considerably (Bae et al., 2023; Nah et al., 2023; Zhang et al., 2022), which in turn affects aerosol pH. Variation in pH would influence the formations of $PM_{2.5}$ via affecting the gas-particle partitioning of semi-volatile species (e.g. HNO_3) and chemical kinetics, thereby feeding back into the air quality, climate and human health (Cheng et al., 2016; Li et al., 2017; Pye et al., 2020; Su et al., 2020).

The recently proposed multiphase buffer theory offers a new quantitative insight into the aforementioned issue, which shows how and why the chemical profiles and meteorological parameters would influence the aerosol acidity(Zheng et al., 2020, 2022a, 2024b). Here, we established a hierarchical influencing factor relationship of

https://doi.org/10.5194/egusphere-2024-3584
Preprint. Discussion started: 29 November 2024

aerosol pH based on the multiphase buffer theory with interpretive structural modelling approach (ISM). Combining this model with time series analysis, we proposed a new hierarchical quantitative analysis framework to quantify driving factors, and applied it to the long-term observations in Changzhou, China. Distinct driving factors were found for pH variations across different time series components, the underlying mechanisms were quantified, and future implications were also discussed.

2. Methods

2.1 Ambient measurements and aerosol acidity prediction

Long-term observations of aerosol chemical components and precursor gases are conducted at an urban site of Changzhou Environmental Monitoring Center (31.76° N, 119.96° E), which is located in Changzhou, an important city in the center of Yangtze River Delta (YRD) region. Further details regarding the sampling site and instruments information are described elsewhere(Li et al., 2023; Yi et al., 2022). Briefly, the $PM_{2.5}$ is measured by a Continuous Particulate Matter Monitor (BAM1020, Met One Inc., US) using β-ray technology, and the meteorological parameters are obtained from a meteorological monitor (WXT520, VAISALA Inc., FL). The water-soluble inorganic ions and the gas species, including NH_3, HNO_3, and HCl, etc., are measured by a MARGA ion online analyzer (ADI2080, Metrohm Inc., CHN). Here the data from 2018 to 2023 are analyzed.

The thermodynamic model ISORROPIA v2.3 (Fountoukis and Nenes, 2007) is employed to predict the aerosol water content (AWC) and aerosol acidity, which is defined as the free molality of protons (Fountoukis and Nenes, 2007; Pye et al., 2020). Input parameters include SO_4^{2-}, total nitrate (gas HNO_3 + particle NO_3^-), total ammonia (gas NH_3 + particle NH_4^+), total chloride (gas HCl + particle Cl^-), NVCs and meteorological parameters like the temperature *T* and relative humidity RH. The ISORROPIA model is run in the forward mode and metastable state (Zheng et al., 2022b).

The ISORROPIA-predicted concentrations of NH_3, NH_4^+ and NO_3^- agreed well with measurements (R^2 all above 0.95 and slopes all close to 1.0; Fig.S1). This demonstrate that thermodynamic analysis accurately reflects the aerosol state. However, the predicted HNO_3 concentration does not correlate well with the observed concentrations, as has been observed in many other studies (Ding et al., 2019; Zhou et al., 2022). This discrepancy may be attributed to the high measurement uncertainty of gas-phase HNO_3 due to its low concentration (Rumsey et al., 2014).

https://doi.org/10.5194/egusphere-2024-3584
Preprint. Discussion started: 29 November 2024

2.2 Time series analysis

Time series analysis is a statistical method of analyzing a sequence of data points over an interval of time, which is particularly useful for understanding the structure and pattern of temporal data and is widely applied in atmospheric studies(Shumway and Stoffer, 2017) (Hammer et al., 2020; Kang et al., 2020). Here, we performed time series analysis of pH and its potential influencing factors by decomposing them into 4 components: long-term trends, seasonal variations, diurnal cycles and random residues. Linear-fitting is adopted to predict the long-term trends (Kang et al., 2020; Mudelsee, 2019), and one-term Fourier curve fitting is adopted to fit the seasonal and diurnal cycles (Bloomfield, 2004; Singh et al., 2017). Here, we fixed the cycle period of Fourier curve as 1 year and 1 day in fitting the seasonal and diurnal variations, respectively. The random residues were obtained from the difference between the actual observed values and the sum of the predicted values of fitting functions in long-term trend, seasonal variations and diurnal cycles.

2.3 Variation contribution quantification

To quantify the contribution of a direct influencing factor to the variations of a certain term, the one-at-a-time sensitivity analysis method is adopted (Yu et al., 2019). Briefly, assume variable Y is a function of n influencing factors of x_1 to x_n, i.e. $Y = f(x_1, \ldots, x_n)$. The variations in Y due to factor x_i, $\partial Y/\partial x_i$, is estimated as:

$$\partial Y/\partial x_i = f(\bar{x}_1, \ldots, x_i, \ldots, \bar{x}_n) - f(\bar{x}_1, \ldots, \bar{x}_n) \quad (1)$$

where x_i is the actual value of factor x_i, and $\bar{x}_i$ is the average of factor x_i. See more details in SI Text S1.

3. Establishing the new hierarchical quantitative analysis framework

3.1 Interpretive structural model (ISM) based on multiphase buffer theory

The recently proposed multiphase buffer theory reveals that most continental regions are within the ammonia-buffered regime, where the pH variations can be decomposed into(Zheng et al., 2020, 2022a):

$$\mathrm{pH} = \mathrm{p}K_a^* + c_{ni} + \mathrm{X}_{gp} \quad (2a)$$

where

$$K_a^* = K_{a,NH_3} \frac{\rho_w}{H_{NH_3} R\, T\, AWC} \quad (2b)$$

$$c_{ni} = log \frac{\gamma_{H^+}}{\gamma_{NH_4^+}} \quad (2c)$$

https://doi.org/10.5194/egusphere-2024-3584
Preprint. Discussion started: 29 November 2024

$$X_{gp} = log\frac{[NH_3(g)]}{[NH_4^+(aq)]} \quad (2d)$$

Here, K_a^* is the effective acid dissociation constant of NH_3 under ideal conditions in multiphase systems, c_{ni} is the non-ideality correction factor, and X_{gp} represents the gas-particle partitioning of NH_3. The $K_{a,\ NH3}$ is acid dissociation constant of NH_3 in bulk aqueous phase, ρ_w is the water density, H_{NH_3} is Henry's law constant of NH_3, R is the gas constant, T is temperature in K, and γ_X is the activity coefficient of X.

Each term of the top-level pH decompositions (Eq. 2a) further depends on many other influencing factors, making the overall picture complicated. To illustrate the interconnections among these multiple driving factors, we applied the interpretive structural modeling (ISM) approach, which is widely used to identify and analyze the relationships between factors in complex systems (Sushil, 2012; Thakkar, 2021). With this method, a hierarchical relationship among influencing factors of aerosol pH can be established based on the multiphase buffer theory, as illustrated in Figure 1. Take the pK_a^* for illustration. The pK_a^* makes a direct impact on pH (top-level influencing factor), and its variation is determined by temperature and AWC. The AWC further depends mainly on $PM_{2.5}$ concentrations and RH, and minorly on the chemical profiles (middle level). Fundamentally, these influencing factors are caused by variations in synoptic conditions and emissions (bottom level).

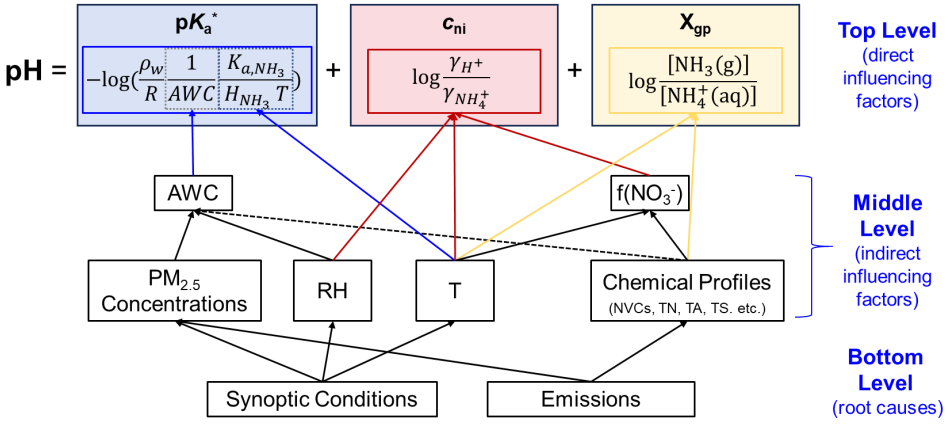

Figure 1: Hierarchical relationship among influencing factors of aerosol pH based on the multiphase buffer theory as established with the interpretive structural modeling approach.

https://doi.org/10.5194/egusphere-2024-3584
Preprint. Discussion started: 29 November 2024

3.2 ISM coupled with the time series analysis

With the above ISM model, a quantitative analysis of each factor following the influencing lines can be achieved. In addition, when coupled with the time series analysis, it can be applied to illustrate the driving factor of each time series component. Briefly, we can decompose each input parameter in ISORROPIA v2.3 into the 4 time series components (sect. 2.1 and 2.2), and then apply each component to explain upper-level factors of corresponding component. For example, the seasonal variations in Y due to seasonal variations of factor x_i, $\partial Y/\partial x_i|_{seas}$, is estimated as:

$$\partial Y/\partial x_i|_{seas} = f(\bar{x}_1, \ldots, x_{i,\,seas} + \bar{x}_i, \ldots, \bar{x}_n) - f(\bar{x}_1, \ldots, \bar{x}_n) \quad (3)$$

Where $x_{i,\,seas}$ is the decomposed seasonal variation of x_i. See more details in SI of Text S2.

4. Driving factor analysis of long-term data in Changzhou

Here we applied the new framework (sect. 3) to analyze the long-term data in Changzhou. From 2018 to 2023, around 90% periods are within the ammonia-buffered regime, while the rest are due to low RH (< 0.3) and aerosols not in a fully deliquescent state. Thus, the drivers of pH can be explained with the above framework.

The top-level ISM decomposition shows that the pH variations are mainly driven by the pK_a^* (~52%) and c_{ni} (~36%), while the X_{gp} varies to a less extent (~12%, Figs. 2a and S2). In comparison, the time-series decomposition indicates that the pH variation is predominantly driven by seasonal variations and random residues, while the long-term trend and diurnal cycle play minor roles on the variations (Fig. 2b). Below we analyzed the driving factors of each time series component.

https://doi.org/10.5194/egusphere-2024-3584
Preprint. Discussion started: 29 November 2024

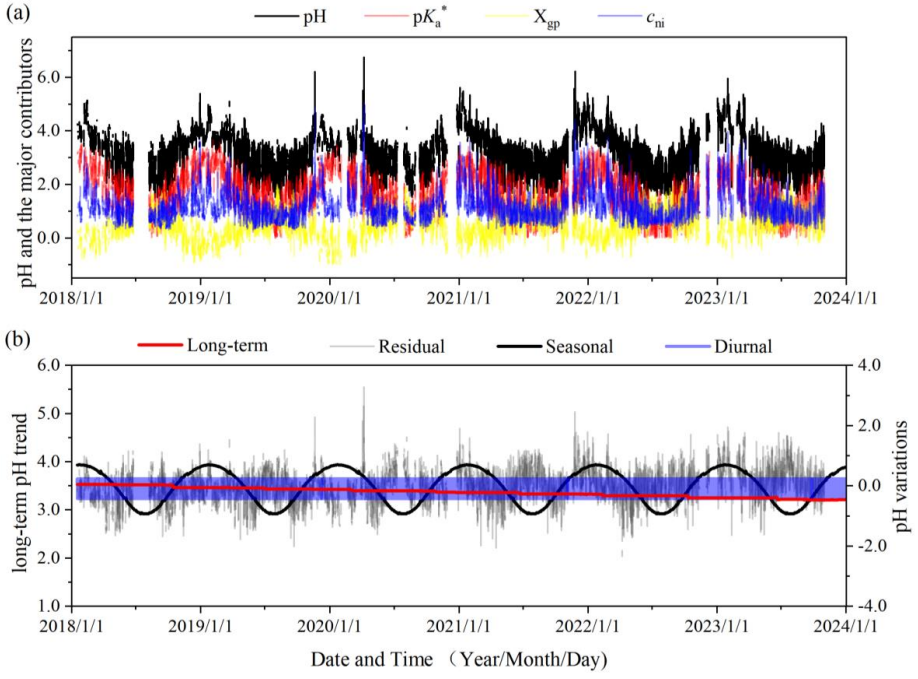

Figure 2: Major components of pH variations. (a) Decomposition into the pK_a^*, X_{gp} and c_{ni} base on the multiphase buffer theory. (b) Decomposition into long-term trends (left axis), seasonal variations, diurnal cycles and residuals (right axis) through time series analysis.

4.1 Long-term trends

The long-term pH trends in Changzhou show a slight decreasing trend of -0.05 year^{-1} (Fig. 2b). The top-level ISM decompositions reveal that this is due to the competing trends of pK_a^* and c_{ni} with X_{gp}: while pK_a^* and c_{ni} decreased by -0.12 year^{-1} and -0.14 year^{-1}, respectively, the X_{gp} increased by 0.21 year^{-1} (Fig. 3a).

https://doi.org/10.5194/egusphere-2024-3584
Preprint. Discussion started: 29 November 2024

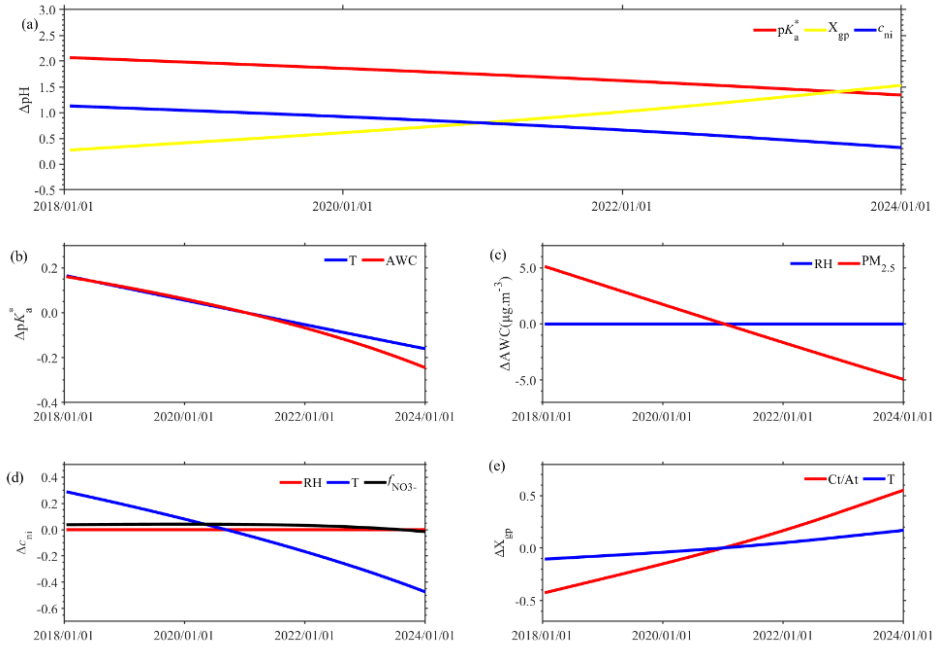

Figure 3: Influencing factors of long-term pH variation at different levels. (a) The 1st level decomposition into pK_a^*, X_{gp} and c_{ni}. (b)-(e) Further investigation of the influencing factors of (b) pK_a^* due to T and AWC, (c) AWC due to RH and $PM_{2.5}$, (d) c_{ni} due to RH, T, $f_{NO_3^-}$, and (e) X_{gp} due to C_t/A_t and T.

A further delve into the middle-level factors in the ISM reveals that the pK_a^* decrease is due to the combined effect of decreasing AWC and increasing temperature (Fig. 3b). The temperature increased by 0.74 K· year^{-1} (Fig. S3), corresponding to a pK_a^* of -0.05 year^{-1}. In comparison, the AWC exhibited a decrease of -1.57 μg·m^{-3}·year^{-1} (Fig. S3), corresponding to a pK_a^* of -0.07 year^{-1}. The AWC decrease is primarily attributed to the $PM_{2.5}$ decrease (around -1.6 μg·m^{-3}·year^{-1}), while the long-term RH shows minimal variation (Fig. 3c). As to c_{ni}, its decreasing trend is mainly attributed to increased temperature, corresponding to c_{ni} of -0.13 year^{-1} (Fig. 3d). RH and $f_{NO_3^-}$ cause negligible effects on c_{ni} because they were nearly constant (Fig. S3). In terms of X_{gp}, its increase is due to the increase in both relative abundance of alkaline to acidic substances (C_t/A_t) and temperature (Fig. 3e), contributing to the X_{gp} increases of 0.16 year^{-1} and 0.05 year^{-1}, respectively. Here the temperature influences X_{gp} through the gas-particle partitioning volatility of semi-volatile species like ammonium nitrate. The increase in C_t/A_t is further due to a much larger decrease in A_t (sulfate, total nitrate, total chloride, etc.) than C_t (total ammonia and NVCs, etc.) (Fig. S3).

https://doi.org/10.5194/egusphere-2024-3584
Preprint. Discussion started: 29 November 2024

Overall, we see that the long-term pH trend shows only a slight decrease despite considerable emission changes during this period, which is a combined effect of decreased $PM_{2.5}$ while increased temperature and C_l/A_t.

4.2 Seasonal variations

Influencing factors of seasonal variation pH are analyzed in similar ways with the long-term trends (**Error! Reference source not found.**). Overall, the pH is higher in winter and spring than summer and autumn, with the amplitude of seasonal variations being 0.81, or the variation range being 1.62. The extent of variation is quantified by variation range hereinafter, which is the difference between the highest and lowest values for a given variable and for a given time series component. This cycle is consistent with pK_a^* and c_{ni} while in reverse phase with the X_{gp}.

The middle-level ISM decompositions demonstrate that the seasonal variation of pK_a^* is mainly driven by the temperature (Fig. 4b). The variation of temperature is 23.26 K (Fig. S4), which corresponds to a pK_a^* variation of 1.20. In comparison, AWC varies to a less extent seasonally (Fig. S4), causing a relatively minor variation of 0.42 in pK_a^*. Seasonal variation of AWC is further primarily attributed to the variation in $PM_{2.5}$ levels (approximately 25.4 $\mu g \cdot m^{-3}$), as the seasonal RH varied little (Fig. 4c and Fig. S4). As to X_{gp}, its seasonal variation is influenced by both temperature and C_l/A_t, which correspond to the variations in X_{gp} of -0.98 and -0.91, respectively (Fig. 4d). Higher temperature and C_l/A_t during summer facilitate more NHx to remain in the gas phase than winter (Fig. S4). Regarding c_{ni}, its seasonal variation is attributable to the combined effects of temperature and $f_{NO_3^-}$ (Fig.4e), leading to variations in c_{ni} of 1.25 and 0.54, respectively. Again, influence of RH is negligible due to its little variations (Fig.4e). The seasonal variations of $f_{NO_3^-}$ is governed by significant variations of temperature (Fig. 4f). Temperature in winter is low enough and causes the vast majority of total nitrate to partition into the particle phase, leading to minor variation of $f_{NO_3^-}$ with temperature variations (Fig.S5). Conversely, higher temperatures in summer result in more total nitrate existing as HNO_3 and $f_{NO_3^-}$ is sensitive to temperature variations.

https://doi.org/10.5194/egusphere-2024-3584
Preprint. Discussion started: 29 November 2024

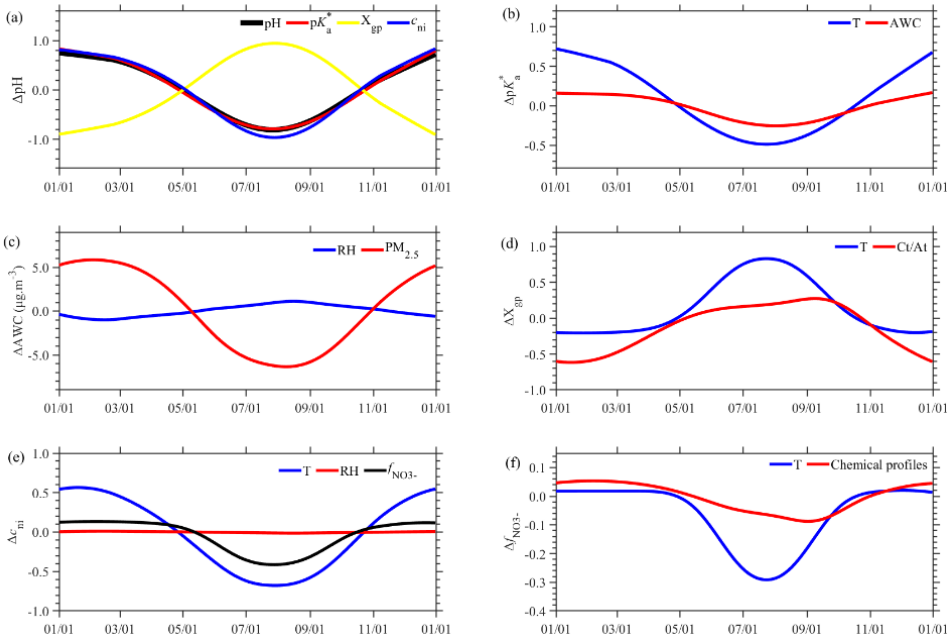

Figure 4: Influencing factors of the seasonal variations of aerosol pH. (a) The 1st level decomposition into pK_a^*, X_{gp} and c_{ni}. (b)-(f) Further investigation of the influencing factors of (b) pK_a^* due to T and AWC, (c) AWC due to RH and $PM_{2.5}$, (d)X_{gp} due to C_t/A_t and T, (e) c_{ni} due to RH, T, $f_{NO_3^-}$, and (f) $f_{NO_3^-}$ due to T and chemical profiles.

Overall, we see that the large seasonal variation of pH is mainly driven by the temperature as it plays a dominant role in both pK_a^*, c_{ni} and X_{gp} (74%, 89% and 52%, respectively). In comparison, net influence of chemical profiles is relatively smaller, contributing 48% and 10% to X_{gp} and c_{ni}, respectively. That is, the seasonal variation of pH is largely driven by the meteorology (esp. temperature) rather than emissions.

4.3 Diurnal cycles

Diurnal cycles of pH are higher at nighttime than daytime, with a variation range of 0.65. Similar to the seasonal variations, the diurnal cycle is also consistent with pK_a^* and c_{ni} trend while in reverse trend with the X_{gp} (Fig. S6a), with their contribution to pH being 0.70, 0.58 and -0.63, respectively.

The major driving factors of diurnal cycles in pK_a^* is different with that of seasonal variations. First, the diurnal cycles of pK_a^* is driven by both AWC (0.45) and temperature (0.25) (Fig. S6b), in contrast to the dominance of temperature in seasonal variations (sect. 4.2). This is mainly due to the much smaller temperature variation range diurnally (4.87 K; Fig. S7) than that seasonally (23.26 K). In addition, diurnal variation of AWC is primarily

https://doi.org/10.5194/egusphere-2024-3584
Preprint. Discussion started: 29 November 2024

influenced by RH (Fig. S6c) due to the larger RH diurnal variations (0.16 versus 0.03 in seasonal variations; Fig. S7 and S4), in contrast with the $PM_{2.5}$ dominance in seasonal variations. In terms of X_{gp}, its dominant driving factor of diurnal cycles is C_t/A_t, in contrast with the dominance of temperature in seasonal variations (Fig. S6d). Diurnal cycles of c_{ni} are due to the combined effects of temperature and $f_{NO_3^-}$ (Fig. S6e), where the $f_{NO_3^-}$ are further mainly driven by chemical profiles (Fig. S6f).

4.4 Residual

The random residual of aerosol pH is another major contributor to pH temporal variations, which is comparable with the seasonal variations. Distinct from all the three components above, the largest top-level contributor to random residuals turns out to be c_{ni} (82%), even exceeding that of pK_a^* (42%), while X_{gp} causes a net negative effect (-24%; Fig. S8). Moreover, random fluctuations of c_{ni} are almost entirely due to variations in $f_{NO_3^-}$ (~95%; Fig. 5a), which are primarily driven by chemical profiles (~93%; Fig. 5b). The pK_a^* random fluctuations are mainly caused by AWC (~79%), which is further attributed mainly (~60%) to $PM_{2.5}$ variations (Fig. 5d). Random variations of X_{gp} are dominated by the chemical profiles, similar to diurnal cycles and long-term trend (Fig.S9). Overall, $PM_{2.5}$ and chemical profiles are the major influencing factors for random residual of pH, underscoring the prominence of emissions over meteorology.

https://doi.org/10.5194/egusphere-2024-3584
Preprint. Discussion started: 29 November 2024

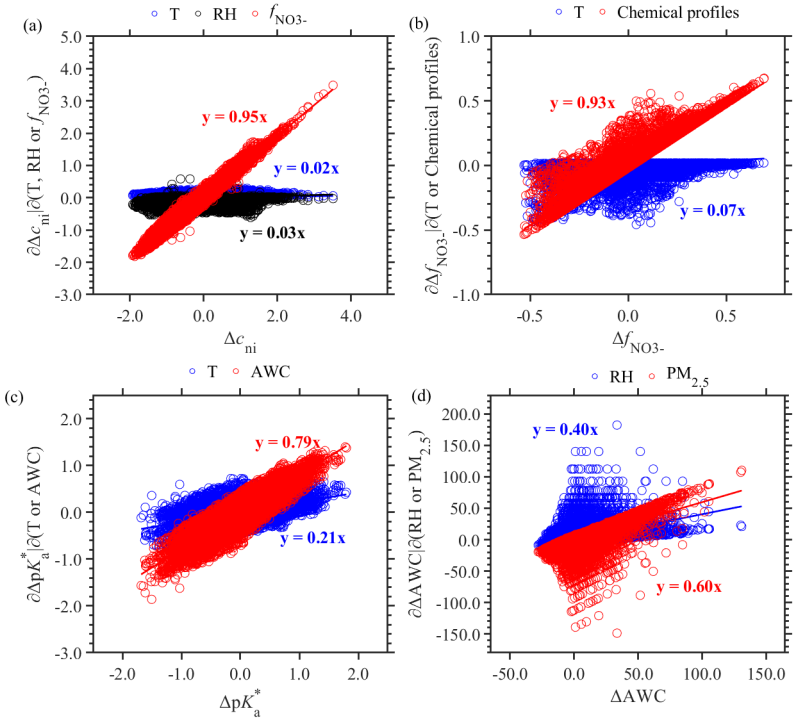

Figure 5: Influencing factors of the random residual of aerosol pH. (a) c_{ni} due to T, RH, and $f_{NO_3^-}$, (b) $f_{NO_3^-}$ due to T and Chemical profiles, (c) pK_a^* due to T and AWC, (d) AWC due to RH and $PM_{2.5}$.

5. Overall contributions and implications

Figure 6 shows the distinct major influencing factors of aerosol pH in the 4 time series components, where the factors contributing less than |10%| are not shown. Overall, pK_a^* is the dominant influencing factor of pH variations, being the major contributor in all components, and playing a pivotal role in seasonal and diurnal cycles (Fig. 6). The c_{ni} is another dominant factor for pH variations, especially in random fluctuations. The X_{gp} shows a reverse trend with pH in all components. As seasonal and random variations largely regulate the pH temporal variations, the pK_a^* and c_{ni} contribute more to pH than X_{gp}.

https://doi.org/10.5194/egusphere-2024-3584
Preprint. Discussion started: 29 November 2024

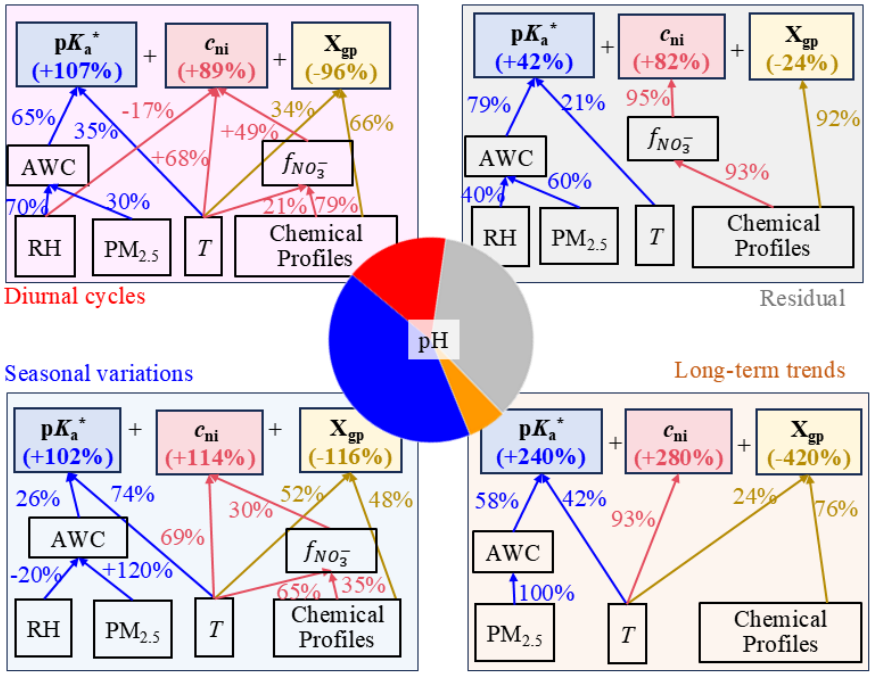

Figure 6: Hierarchical relationship among major influencing factors of aerosol pH during 4 time series (Factors contributing less than |10%| are not shown)**.**

Deeper-level driver analysis show that meteorology plays a more important role than chemical profiles in explaining the pH temporal variations (57% versus 22%; Fig. S10). Temperature is the major contributor, which explains seasonal variations in pK_a^*, c_{ni}, and X_{gp} of 74%, 89% and 52%, respectively, and it is also important in diurnal cycles and long-term trends. RH plays an important role in diurnal cycles, accounting for 70% of the AWC diurnal variations and thus indirectly exerting an important effect on pK_a^* (~46%). In comparison, chemical profiles are essential for explaining long-term trends in X_{gp}, and they also provide a pivotal role in random fluctuations and diurnal cycles for c_{ni}. The $PM_{2.5}$ concentration is an overall effect of meteorology and emissions. $PM_{2.5}$ is the dominant contributor to AWC in all components except diurnal cycles, exerting an indirect influence on pK_a^*. Overall, temperature is critical in explaining pH variations (48%; Fig. S10), followed by chemical profiles, $PM_{2.5}$ concentrations and RH (22%, 21% and 9%, respectively).

The quantitative framework we proposed here can provide a clear understanding of the drivers of aerosol acidity temporal variations, with information on both quantitative contributions and the underlying mechanisms. Our

https://doi.org/10.5194/egusphere-2024-3584
Preprint. Discussion started: 29 November 2024

findings suggest that relative importance of synoptic conditions versus emissions in aerosol acidity variations differed much with the time scale of concern and are through different major mechanisms. In Changzhou, synoptic conditions are more important for seasonal variations and diurnal cycles of pH, while emissions cause greater effect on pH random fluctuations. For the long-term trends, both emissions and synoptic conditions are important. In other places, this framework still applies, while the conclusions may vary. These quantitative understandings on the driving factors of aerosol acidity are important in acidity-relevant process studies and policy-making, such as nitrate control(Guo et al., 2017), sulfate formation(Cheng et al., 2016; Zheng et al., 2024a), nitrogen depositions (Nenes et al., 2021), etc.

Data availability. The dataset of aerosol chemical components and precursor gases is available on the website http://192.168.100.25/czems/MainFrame.aspx supported by Changzhou Ecological Environment Bureau.

Author contributions. G.Z. and Q. Zhang designed and led the study. X. D., G.Z. and C. Chen performed the study. C. Chen conducted the campaign and collected the data. X. D. and G.Z. wrote the manuscript with the input of all authors. All authors have given approval to the final version of the manuscript.

Competing interests. At least one of the (co-)authors is a member of the editorial board of Atmospheric Chemistry and Physics.

Acknowledgments. The research was supported by the National Natural Science Foundation of China (22188102). C. Chen thanks the Shuimu Tsinghua Scholar Program (2023SM027).

References

Bae, M., Kang, Y.-H., Kim, E., Kim, S., and Kim, S.: A multifaceted approach to explain short- and long-term PM2.5 concentration changes in Northeast Asia in the month of January during 2016–2021, Science of The Total Environment, 880, 163309, https://doi.org/10.1016/j.scitotenv.2023.163309, 2023.

Bloomfield, P.: Fourier Analysis of Time Series: An Introduction, John Wiley & Sons, 285 pp., 2004.

Cheng, Y., Zheng, G., Wei, C., Mu, Q., Zheng, B., Wang, Z., Gao, M., Zhang, Q., He, K., Carmichael, G., Pöschl, U., and Su, H.: Reactive nitrogen chemistry in aerosol water as a source of sulfate during haze events in China, Sci. Adv., 2, e1601530, https://doi.org/10.1126/sciadv.1601530, 2016.

Clegg, S. L., Seinfeld, J. H., and Brimblecombe, P.: Thermodynamic modelling of aqueous aerosols containing

https://doi.org/10.5194/egusphere-2024-3584
Preprint. Discussion started: 29 November 2024

electrolytes and dissolved organic compounds, Journal of Aerosol Science, 32, 713–738, https://doi.org/10.1016/S0021-8502(00)00105-1, 2001.

Ding, J., Zhao, P., Su, J., Dong, Q., Du, X., and Zhang, Y.: Aerosol pH and its driving factors in Beijing, Atmos. Chem. Phys., 19, 7939–7954, https://doi.org/10.5194/acp-19-7939-2019, 2019.

Fountoukis, C. and Nenes, A.: ISORROPIA II: a computationally efficient thermodynamic equilibrium model for K +–Ca2+–Mg2+–NH+ 4 –Na+–SO2− 4 –NO− 3 –Cl−–H2O aerosols, Atmos. Chem. Phys., 4639–4659, 2007.

Guo, H., Liu, J., Froyd, K. D., Roberts, J. M., Veres, P. R., Hayes, P. L., Jimenez, J. L., Nenes, A., and Weber, R. J.: Fine particle pH and gas–particle phase partitioning of inorganic species in Pasadena, California, during the 2010 CalNex campaign, Atmos. Chem. Phys., 17, 5703–5719, https://doi.org/10.5194/acp-17-5703-2017, 2017.

Hammer, M. S., Van Donkelaar, A., Li, C., Lyapustin, A., Sayer, A. M., Hsu, N. C., Levy, R. C., Garay, M. J., Kalashnikova, O. V., Kahn, R. A., Brauer, M., Apte, J. S., Henze, D. K., Zhang, L., Zhang, Q., Ford, B., Pierce, J. R., and Martin, R. V.: Global Estimates and Long-Term Trends of Fine Particulate Matter Concentrations (1998–2018), Environ. Sci. Technol., 54, 7879–7890, https://doi.org/10.1021/acs.est.0c01764, 2020.

Kang, Y.-H., You, S., Bae, M., Kim, E., Son, K., Bae, C., Kim, Y., Kim, B.-U., Kim, H. C., and Kim, S.: The impacts of COVID-19, meteorology, and emission control policies on PM2.5 drops in Northeast Asia, Sci Rep, 10, 22112, https://doi.org/10.1038/s41598-020-79088-2, 2020.

Li, Q., Zhang, K., Li, R., Yang, L., Yi, Y., Liu, Z., Zhang, X., Feng, J., Wang, Q., Wang, W., Huang, L., Wang, Y., Wang, S., Chen, H., Chan, A., Latif, M. T., Ooi, M. C. G., Manomaiphiboon, K., Yu, J., and Li, L.: Underestimation of biomass burning contribution to PM2.5 due to its chemical degradation based on hourly measurements of organic tracers: A case study in the Yangtze River Delta (YRD) region, China, Science of The Total Environment, 872, 162071, https://doi.org/10.1016/j.scitotenv.2023.162071, 2023.

Li, W., Xu, L., Liu, X., Zhang, J., Lin, Y., Yao, X., Gao, H., Zhang, D., Chen, J., Wang, W., Harrison, R. M., Zhang, X., Shao, L., Fu, P., Nenes, A., and Shi, Z.: Air pollution–aerosol interactions produce more bioavailable iron for ocean ecosystems, Sci. Adv., 3, e1601749, https://doi.org/10.1126/sciadv.1601749, 2017.

Mudelsee, M.: Trend analysis of climate time series: A review of methods, Earth-Science Reviews, 190, 310–322, https://doi.org/10.1016/j.earscirev.2018.12.005, 2019.

Nah, T., Lam, Y. H., Yang, J., and Yang, L.: Long-term trends and sensitivities of PM2.5 pH and aerosol liquid water to chemical composition changes and meteorological parameters in Hong Kong, South China: Insights from

https://doi.org/10.5194/egusphere-2024-3584
Preprint. Discussion started: 29 November 2024

10-year records from three urban sites, Atmospheric Environment, 302, 119725, https://doi.org/10.1016/j.atmosenv.2023.119725, 2023.

Nenes, A., Pandis, S. N., Kanakidou, M., Russell, A. G., Song, S., Vasilakos, P., and Weber, R. J.: Aerosol acidity and liquid water content regulate the dry deposition of inorganic reactive nitrogen, Atmos. Chem. Phys., 21, 6023–6033, https://doi.org/10.5194/acp-21-6023-2021, 2021.

Pye, H. O. T., Nenes, A., Alexander, B., Ault, A. P., Barth, M. C., Clegg, S. L., Collett Jr., J. L., Fahey, K. M., Hennigan, C. J., Herrmann, H., Kanakidou, M., Kelly, J. T., Ku, I.-T., McNeill, V. F., Riemer, N., Schaefer, T., Shi, G., Tilgner, A., Walker, J. T., Wang, T., Weber, R., Xing, J., Zaveri, R. A., and Zuend, A.: The acidity of atmospheric particles and clouds, Atmos. Chem. Phys., 20, 4809–4888, https://doi.org/10.5194/acp-20-4809-2020, 2020.

Rumsey, I. C., Cowen, K. A., Walker, J. T., Kelly, T. J., Hanft, E. A., Mishoe, K., Rogers, C., Proost, R., Beachley, G. M., Lear, G., Frelink, T., and Otjes, R. P.: An assessment of the performance of the Monitor for AeRosols and GAses in ambient air (MARGA): a semi-continuous method for soluble compounds, Atmos. Chem. Phys., 14, 5639–5658, https://doi.org/10.5194/acp-14-5639-2014, 2014.

Shumway, R. H. and Stoffer, D. S.: Time Series Analysis and Its Applications: With R Examples, Springer International Publishing, Cham, https://doi.org/10.1007/978-3-319-52452-8, 2017.

Singh, P., Joshi, S. D., Patney, R. K., and Saha, K.: The Fourier decomposition method for nonlinear and non-stationary time series analysis, Proc. R. Soc. A., 473, 20160871, https://doi.org/10.1098/rspa.2016.0871, 2017.

Su, H., Cheng, Y., and Pöschl, U.: New Multiphase Chemical Processes Influencing Atmospheric Aerosols, Air Quality, and Climate in the Anthropocene, Acc. Chem. Res., 53, 2034–2043, https://doi.org/10.1021/acs.accounts.0c00246, 2020.

Sushil: Interpreting the Interpretive Structural Model, Glob J Flex Syst Manag, 13, 87–106, https://doi.org/10.1007/s40171-012-0008-3, 2012.

Tao, Y. and Murphy, J. G.: The sensitivity of PM2.5 acidity to meteorological parameters and chemical composition changes: 10-year records from six Canadian monitoring sites, Atmospheric Chemistry and Physics, 19, 9309–9320, https://doi.org/10.5194/acp-19-9309-2019, 2019.

Tao, Y. and Murphy, J. G.: Simple Framework to Quantify the Contributions from Different Factors Influencing Aerosol pH Based on NHx Phase-Partitioning Equilibrium, Environ. Sci. Technol., 55, 10310–10319, https://doi.org/10.1021/acs.est.1c03103, 2021.

https://doi.org/10.5194/egusphere-2024-3584
Preprint. Discussion started: 29 November 2024

Thakkar, J. J.: Multi-Criteria Decision Making, Springer Singapore, Singapore, https://doi.org/10.1007/978-981-33-4745-8, 2021.

Tilgner, A., Schaefer, T., Alexander, B., Barth, M., Collett Jr., J. L., Fahey, K. M., Nenes, A., Pye, H. O. T., Herrmann, H., and McNeill, V. F.: Acidity and the multiphase chemistry of atmospheric aqueous particles and clouds, Atmos. Chem. Phys., 21, 13483–13536, https://doi.org/10.5194/acp-21-13483-2021, 2021.

Yi, Y., Li, Q., Zhang, K., Li, R., Yang, L., Liu, Z., Zhang, X., Wang, S., Wang, Y., Chen, H., Huang, L., Yu, J. Z., and Li, L.: Highly time-resolved measurements of elements in PM2.5 in Changzhou, China: Temporal variation, source identification and health risks, Science of The Total Environment, 853, 158450, https://doi.org/10.1016/j.scitotenv.2022.158450, 2022.

Yu, S., Yun, S.-T., Hwang, S.-I., and Chae, G.: One-at-a-time sensitivity analysis of pollutant loadings to subsurface properties for the assessment of soil and groundwater pollution potential, Environ Sci Pollut Res, 26, 21216–21238, https://doi.org/10.1007/s11356-019-05002-7, 2019.

Zaveri, R. A., Easter, R. C., Fast, J. D., and Peters, L. K.: Model for Simulating Aerosol Interactions and Chemistry (MOSAIC), J. Geophys. Res., 113, 2007JD008782, https://doi.org/10.1029/2007JD008782, 2008.

Zhang, L., Zhao, N., Zhang, W., and Wilson, J. P.: Changes in Long-Term PM2.5 Pollution in the Urban and Suburban Areas of China's Three Largest Urban Agglomerations from 2000 to 2020, Remote Sensing, 14, 1716, https://doi.org/10.3390/rs14071716, 2022.

Zheng, G., Su, H., Wang, S., Andreae, M. O., Pöschl, U., and Cheng, Y.: Multiphase buffer theory explains contrasts in atmospheric aerosol acidity, Science, 369, 1374–1377, https://doi.org/10.1126/science.aba3719, 2020.

Zheng, G., Su, H., Wang, S., Pozzer, A., and Cheng, Y.: Impact of non-ideality on reconstructing spatial and temporal variations in aerosol acidity with multiphase buffer theory, Atmos. Chem. Phys., 22, 47–63, https://doi.org/10.5194/acp-22-47-2022, 2022a.

Zheng, G., Su, H., and Cheng, Y.: Revisiting the Key Driving Processes of the Decadal Trend of Aerosol Acidity in the U.S, ACS Environ. Au, 2, 346–353, https://doi.org/10.1021/acsenvironau.1c00055, 2022b.

Zheng, G., Su, H., Andreae, M. O., Pöschl, U., and Cheng, Y.: Multiphase Buffering by Ammonia Sustains Sulfate Production in Atmospheric Aerosols, AGU Advances, 5, e2024AV001238, https://doi.org/10.1029/2024AV001238, 2024a.

Zheng, G., Su, H., Wan, R., Duan, X., and Cheng, Y.: Rising Alkali-to-Acid Ratios in the Atmosphere May Correspond to Increased Aerosol Acidity, Environ. Sci. Technol., https://doi.org/10.1021/acs.est.4c06860, 2024b.

https://doi.org/10.5194/egusphere-2024-3584
Preprint. Discussion started: 29 November 2024

Zhou, M., Zheng, G., Wang, H., Qiao, L., Zhu, S., Huang, D., An, J., Lou, S., Tao, S., Wang, Q., Yan, R., Ma, Y., Chen, C., Cheng, Y., Su, H., and Huang, C.: Long-term trends and drivers of aerosol pH in eastern China, Atmos. Chem. Phys., 22, 13833–13844, https://doi.org/10.5194/acp-22-13833-2022, 2022.

Zuend, A., Marcolli, C., Luo, B. P., and Peter, T.: A thermodynamic model of mixed organic-inorganic aerosols to predict activity coefficients, Atmos. Chem. Phys., 2008.